The Journal of Experimental Biology 204, 1153–1166 (2001)
Printed in Great Britain © The Company of Biologists Limited 2001
JEB3215

GLIDING FLIGHT IN A JACKDAW: A WIND TUNNEL STUDY

MIKAEL ROSÉN* AND ANDERS HEDENSTRÖM
Department of Animal Ecology, Lund University, Ecology Building, SE-223 62 Lund, Sweden
*e-mail: mikael.rosen@zooekol.lu.se

Accepted 18 December 2000; published on WWW 26 February 2001

Summary

We examined the gliding flight performance of a jackdaw *Corvus monedula* in a wind tunnel. The jackdaw was able to glide steadily at speeds between 6 and 11 m s^{-1}. The bird changed its wingspan and wing area over this speed range, and we measured the so-called glide super-polar, which is the envelope of fixed-wing glide polars over a range of forward speeds and sinking speeds.

The glide super-polar was an inverted U-shape with a minimum sinking speed (V_{ms}) at 7.4 m s^{-1} and a speed for best glide (V_{bg}) at 8.3 m s^{-1}. At the minimum sinking speed, the associated vertical sinking speed was 0.62 m s^{-1}. The relationship between the ratio of lift to drag (L:D) and airspeed showed an inverted U-shape with a maximum of 12.6 at 8.5 m s^{-1}. Wingspan decreased linearly with speed over the whole speed range investigated. The tail was spread extensively at low and moderate speeds; at speeds between 6 and 9 m s^{-1}, the tail area decreased linearly with speed, and at speeds above 9 m s^{-1} the tail was fully furled. Reynolds number calculated with the mean chord as the reference length ranged from 38 000 to 76 000 over the speed range 6–11 m s^{-1}.

Comparisons of the jackdaw flight performance were made with existing theory of gliding flight. We also re-analysed data on span ratios with respect to speed in two other bird species previously studied in wind tunnels. These data indicate that an equation for calculating the span ratio, which minimises the sum of induced and profile drag, does not predict the actual span ratios observed in these birds. We derive an alternative equation on the basis of the observed span ratios for calculating wingspan and wing area with respect to forward speed in gliding birds from information about body mass, maximum wingspan, maximum wing area and maximum coefficient of lift. These alternative equations can be used in combination with any model of gliding flight where wing area and wingspan are considered to calculate sinking rate with respect to forward speed.

Key words: gliding, flight, aerodynamics, super-polar, flight theory, wind tunnel, jackdaw, *Corvus monedula.*

Introduction

Gliding is a comparatively inexpensive flight mode in which a bird covers the aerodynamic cost by losing potential energy. However, the bird needs fuel energy to maintain the force on its wings, by pushing them down and forward, to counteract the force generated by the airflow on the wings and by gravity on the mass. This cost is estimated to be approximately 3–4 times the basal metabolic rate (Hedenström, 1993). Potential energy can be stored by soaring in updrafts of thermals, by powered climbing flight prior to gliding descent or by dynamic soaring in the wind gradient over the sea. Without the use of rising air, active climbing flight or a vertical wind gradient, a gliding bird will inevitably end up on the ground or the sea surface. In a wind tunnel, it is possible to generate updrafts by tilting the air stream, i.e. the tunnel, thereby continuously feeding energy to the gliding bird. In theory and practise, it is therefore possible to have a bird gliding in front of an experimenter for prolonged periods.

Gliding flight has previously been studied in wind tunnels (Pennycuick, 1968; Tucker and Parrot, 1970; Withers, 1981; Spedding, 1987; Tucker, 1987; Tucker, 1992; Tucker and Heine, 1990), with the use of a motorized glider in Africa (Pennycuick, 1971a; Pennycuick, 1971b), by tracking radar (Spaar and Bruderer, 1996; Spaar and Bruderer, 1997) and by range finder (Tucker, 1988; Tucker et al., 1998). However, there is still a need for more studies in which the kinematics is carefully monitored to be able to test the predictions of existing gliding flight theory. In this study, we have examined the gliding flight performance of a passerine, the jackdaw *Corvus monedula*. The aim was to define the so-called glide super-polar of a jackdaw, which is the envelope of all possible fixed-wingspan glide polars (minimum sinking rate with respect to forward airspeed) over a range of forward speeds and sinking speeds (Tucker, 1987; Pennycuick, 1989). The super-polar is the polar obtained if the bird is challenged to perform at its minimum possible glide angle in the tunnel when changing wingspan and wing area. A typical feature of gliding flight is that the bird will flex its wings with increasing forward and sinking speed. Tucker (Tucker, 1987) calculated that, by reducing their wingspan, birds are able to minimise the

total drag. According to this theory, the wingspan should be maximised at low speeds, and at a certain speed the wingspan should be reduced with further increases in forward gliding speed.

We will compare our results with the existing theory for predicting sink rate with respect to forward speed in gliding flight (Pennycuick, 1975; Tucker, 1987; Pennycuick, 1989). These comparisons can be made only when accounting for the differences in body mass and morphology. The wing morphology determines how efficient the bird is at converting potential energy to stay aloft and/or glide for long distances and it also determines how well a bird can take advantage of rising air using thermal or slope soaring.

Theory of gliding flight

All measurements made on our bird refer to steady gliding flight. Hence, all the forces acting on the bird are in equilibrium. In the wind tunnel, this is characterised by the bird being stationary with respect to the surrounding test section. When this criterion is met and the gliding angle and forward speed are known, it is possible to calculate the sinking speed as observed on the bird in the wind tunnel. The following theoretical treatment originates from a study by Pennycuick (Pennycuick, 1968), in which he studied a pigeon *Columba livia* gliding in a wind tunnel. Additional information can be found in Tucker (Tucker, 1987) and Pennycuick (Pennycuick, 1989).

A bird in steady gliding flight moves forward at speed V with a flight path inclined downwards at an angle (θ) relative to the horizontal (Fig. 1). To overcome the aerodynamic forces, the bird sinks at a rate V_s, i.e. expends potential energy, which is equal to:

$$V_s = V\sin\theta\,. \tag{1}$$

The total aerodynamic force, i.e. the resultant of lift and drag, acting on a bird gliding at equilibrium is directed upwards and is equal in magnitude to the bird's weight, i.e. mass times the acceleration due to gravity ($m\boldsymbol{g}$). The aerodynamic force has two components. The first is drag (D), which is directed backwards and parallel to the flight path and is expressed as (see Fig. 1):

$$D = m\boldsymbol{g}\sin\theta\,. \tag{2}$$

The second component is lift (L), which is directed upwards and perpendicular to the flight path and is given by (see Fig. 1):

$$L = m\boldsymbol{g}\cos\theta\,. \tag{3}$$

These two force components, lift and drag, depend on the bird's size, wing morphology and the airspeed. To make the lift and drag independent of size, wing area and speed and comparable between birds, it is common practice to convert them into dimensionless force coefficients. The lift coefficient (C_L) is derived using the equation:

$$C_L = L/(\tfrac{1}{2}\rho S V^2)\,, \tag{4}$$

where $\frac{1}{2}\rho V^2$ is the dynamic pressure, which is dependent on air density (ρ) and the square of speed (V), and S is the lifting surface of the bird; S refers to wing area including the area of the body between the wings (Pennycuick, 1989) unless explicitly stated otherwise.

The lift coefficient varies with the orientation of the wing (such as angle of attack) and with Reynolds number Re (see below for the definition of Re).

Drag components

As indicated above, generation of lift inevitably creates drag. Total drag (D) is usually divided into three components:

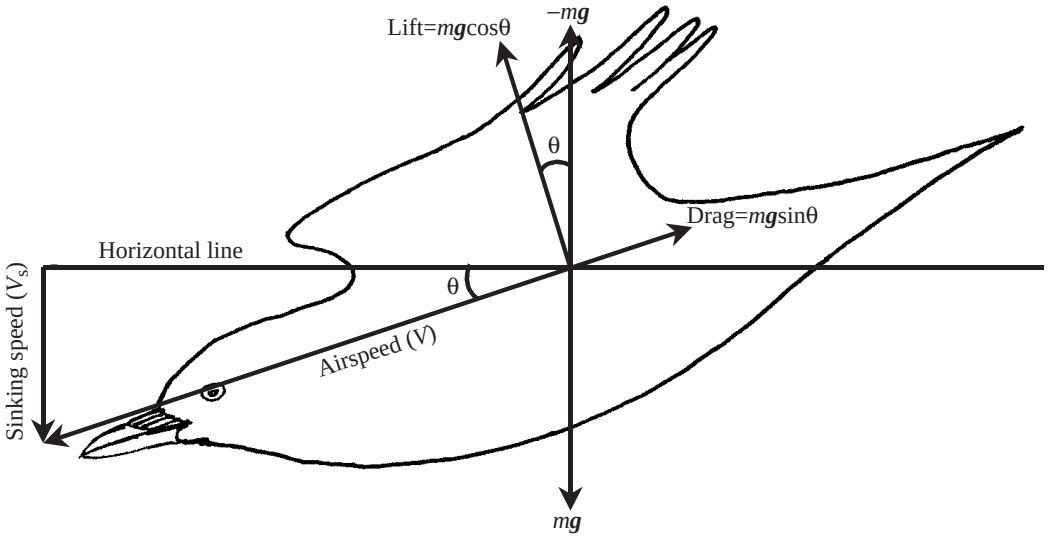

Fig. 1. Forces and speed components for steady gliding flight in a bird. The glide path is inclined downwards relative to the horizontal at an angle θ. Lift is perpendicular to, and drag is parallel to, the glide path. The weight ($m\boldsymbol{g}$) is balanced by the resultant of lift and drag. Airspeed (V) is parallel to the glide path, and sinking speed (V_s) is vertical and positive downwards.

induced drag (D_{ind}), parasite drag (D_{par}) and profile drag (D_{pro}), which are summed:

$$D = D_{ind} + D_{par} + D_{pro} . \quad (5)$$

Induced drag arises when the wings and tail produce the lift required to support the bird's weight. Induced drag is always present when lift is generated because the wing is moving forward and thereby creating an induced downwash. The induced drag of the wings can be written as:

$$D_{ind} = \frac{2kL^2}{\pi\rho b^2 V^2} , \quad (6)$$

where k is the induced drag factor and is a measure of the deviation of the true lift distribution from an ideal elliptical lift distribution (k=1) and b is wingspan. Pennycuick (Pennycuick, 1975; Pennycuick, 1989) assumed a value of k=1.1–1.2 for reasonably efficient wing designs in real birds. The default value for k in gliding flight calculations is usually set at 1.1.

By spreading its tail, a bird can generate an additional aerodynamic force to that of the wings (Hummel, 1992; Tucker, 1992). Thomas (Thomas, 1993) adapted slender lifting surface theory to account for the aerodynamic forces of a bird's tail. To calculate the induced drag of the tail according to this theory, the angle of attack of the tail, among other variables, is required, and we did not measure this for the jackdaw. We have therefore not included the lift and drag generated by the tail explicitly in our aerodynamic calculations.

Parasite drag arises from the form and friction drag of the body. It is proportional to the square of forward speed ($\propto V^2$) and to the cross-sectional frontal area of the bird's body (S_b) at its widest part, excluding the wings. A streamlined body minimises the pressure drag component of parasite drag, i.e. the majority of the drag is due to skin friction, as is the case for some fast-flying birds such as auks, ducks, shorebirds, falcons and swifts. Parasite drag can be written as:

$$D_{par} = \tfrac{1}{2}\rho S_b C_{D,par} V^2 , \quad (7)$$

where $C_{D,par}$ is the parasite drag coefficient that accounts for the skin friction and the form drag of the body. The parasite drag coefficient is treated as a constant in the model proposed by Pennycuick (Pennycuick, 1989), but a change in the orientation of the body, e.g. body tilt angle with respect to speed, will affect the drag of the body.

The wings generate profile drag as they move through the air. Profile drag is a function of wing area, i.e. wing length and chord, and of speed:

$$D_{pro} = \tfrac{1}{2}\rho V^2 S C_{D,pro} , \quad (8)$$

where S is the wing area and $C_{D,pro}$ is the profile drag coefficient, which is assigned a default value of 0.014 for gliding flight (Pennycuick, 1989). The profile drag coefficient varies with the lift coefficient and, therefore, with the orientation of the wing, with speed and with Reynolds number, but over the normal speed range of gliding birds $C_{D,pro}$ is treated as a constant (Pennycuick, 1989). It is assumed that the drag of the bird is the sum of the separate drag components, but there may be an additional interference drag when joining the body and wings. Following others working on gliding flight aerodynamics, we will assume that interference drag is negligible (e.g. Tucker and Heine, 1990). Using the full algebraic expressions for the drag components, adding up to total drag, equation 5 is expanded to:

$$D = \frac{2kL^2}{\pi\rho b^2 V^2} + \tfrac{1}{2}\rho S_b C_{D,par} V^2 + \tfrac{1}{2}\rho V^2 S C_{D,pro} . \quad (9)$$

Variable wingspan

Tucker (Tucker, 1987) showed that, by adjusting wingspan and wing area, a gliding bird could minimise the total drag at different airspeeds. By reducing the wingspan, induced drag will increase, but this will be balanced by a simultaneous reduction in wing area and the associated profile drag. There is an optimum wingspan and area at each speed that minimises the total drag and, hence, gives the minimum rate of sinking. The envelope of all such separate glide polars defines the glide super-polar. Tucker (Tucker, 1987) derived an iterative method to calculate glide super-polars by minimising the total drag of the bird. Pennycuick (Pennycuick, 1989) simplified Tucker's (Tucker, 1987) analysis by minimising the sum of induced and profile drag. From equation 2, it follows that $\sin\theta = D/m\boldsymbol{g}$ which, substituted into equation 1, yields:

$$V_s = \frac{VD}{m\boldsymbol{g}} . \quad (10)$$

This equation can be expanded using equation 9 for drag D. After rearrangement, equation 10 becomes:

$$V_s = \frac{2km\boldsymbol{g}}{\pi\rho b^2 V} + \frac{\rho V^3}{2m\boldsymbol{g}} (S C_{D,pro} + S_b C_{D,par}) , \quad (11)$$

where we have replaced L from equation 9 by $m\boldsymbol{g}$, which is a reasonable approximation at small glide angles θ. When the wing is flexed, the wingspan and wing area are reduced. Let β be the span ratio, defined as actual wingspan b_{obs} divided by the maximum wingspan b_{max}, and let ε be the ratio between actual and maximum wing area S_{max} (*sensu* Pennycuick, 1989). The relationship between ε and β must pass through the point (β,ε)=(1,1) associated with maximum span and area. The few empirical data available suggest that the slope of the relationship (planform slope δ) between ε and β is 1 (see below), and we will therefore assume that ε=β. We then replace b and S in equation 11 with βb and βS, respectively, differentiate V_s with respect to β and set the derivative equal to zero. We solve this equation for β which, after rearranging, gives the following expression for the optimal span ratio $\hat{\beta}$ associated with minimum drag:

$$\hat{\beta} = \left(\frac{8km^2\boldsymbol{g}^2}{\pi\rho^2 b^2 S C_{D,pro} V^4} \right)^{1/3} , \quad (12)$$

where symbols are defined as before. It is anatomically impossible for the wingspan to equal the optimal wingspan

when $\hat{\beta}>1$. Therefore, $\hat{\beta}$ is set to 1 if calculated values are greater than 1, while the calculated values of $\hat{\beta}$ are used when they are less than 1. Tucker's (Tucker, 1987) calculation is aerodynamically a more stringent approach, but the two methods give similar results for span ratios in gliding birds.

Materials and methods

The wind tunnel

The wind tunnel used is of a low-turbulence, closed-circuit type and is situated at the Department of Animal Ecology at Lund University, Sweden. Here, we will only give a brief description of its main features. The reader interested in more details about the design and technical data of this wind tunnel should consult Pennycuick et al. (Pennycuick et al., 1997). The test section is octagonal in cross section, 1.20 m wide and 1.08 m high. The length of the effective test section is approximately 1.8 m, of which the first 1.20 m is covered by acrylic walls and the last 0.5 m is open, giving direct access to the bird. The speed can be varied continuously in the range 0–38 m s^{-1}. The speed range used in this study ranged from 4 to 16 m s^{-1}. The tunnel can also be tilted continuously from horizontal to give 8° descent and 6° climb angles. In this study, we had the tunnel blocked at a maximum descent angle of 6.37°. Note that, even though the speed and tilt angle can be varied continuously, they are read in intervals of 0.1 m s^{-1} and 0.03°, respectively, on the wind tunnel monitor.

Upstream from the test section we mounted a fine net made of braided nylon cord, 0.75 mm in diameter, with a square mesh of 17 mm×17 mm. This net was used throughout the experimental period to prevent the bird from flying into the contraction chamber. The net affects the turbulence level in the test section, as measured by Pennycuick et al. (Pennycuick et al., 1997), which ranges from less than 0.04% (measured as the coefficient of variation in horizontal speed) in the centre of the test section without a net to 1.21% with the net installed.

The jackdaw

A second-year female jackdaw *Corvus monedula* L. was caught at Pildamsparken in Malmö, Sweden, on 18 March 1999. The jackdaw is a partially migrating species, with resident populations in southern Scandinavia, while populations breeding in northern Sweden, Finland and Russia are to a large extent migratory. Jackdaws use both flapping and gliding flight when soaring in the wild and are therefore suitable for studying gliding flight performance.

Food and housing

The jackdaw was kept in an indoor aviary measuring 1.5 m×1.5 m×2 m. On the sides of the aviary, Plexiglas was mounted inside the net walls to prevent the bird from damaging and abrading its feathers. She was allowed 1 week to become accustomed to her new situation and food, which consisted of mealworms and dried dog food dampened with water. Vitamins and minerals were added to the food on a weekly basis.

Flight training

The bird was trained to perch on a stick 1 m long to minimise feather damage and stress. The stick was always used to handle the bird in the tunnel and to transport it between the aviary and the test section of the wind tunnel. Hence, no cuffs, jesses or rings were attached to the bird. In total, the flight training lasted 1 week before the experiments started. At first, the bird just sat on the stick in the test section with only a very low airspeed turned on, to generate the diagnostic sound of the fan. She very quickly became accustomed to the new situation. The first flights were performed with the tunnel in the horizontal position; the bird was gently tossed off the stick at a moderate wind speed (approximately 8 m s^{-1}) and shortly after allowed to land on the stick again. The time between tossing the bird off the stick and letting it land again was increased in a stepwise manner. After a few days, the bird would fly actively for 30 min or more without resting. During flight, the bird was stable and did not appear stressed, as indicated by a closed bill, fully retracted feet and the head retracted towards the body. A wary bird keeps its head erect and stabilised relative to its surroundings, whereas the body moves up and down, features typical of manoeuvring flight. Furthermore, our experience of stressed birds is that their bill is open and their legs are outstretched, held in a position similar to that before landing. None of these features was observed in the jackdaw after a few days of acclimation and training.

The next step was to tilt the tunnel to offer the bird an opportunity to glide. At the first attempt, she started to glide for periods of a few seconds without any encouragement from the experimenter. This period was then gradually elongated and lasted close to 1 min when the bird was fully trained. The bird did not always glide steadily, but started far back in the tunnel test section and glided forward. However, every gliding sequence contained periods of stable gliding in the test section.

Our definition of equilibrium gliding is that the bird remains stationary ('freezes') in the air stream with no movement with respect to the wind tunnel test section. Whether the bird was still or not was judged by eye and by examining filmed sequences captured with a digital video camera. However, since the jackdaw is a fairly large bird, such movement was clearly visible by eye. We define steady gliding as a sequence of gliding lasting at least 5 s. The longest steady glides observed during an experiment lasted up to 60 s, but the average glide duration was near 10 s.

Morphology

Wingspan and wing area were measured as described by Pennycuick (Pennycuick, 1989). Maximum wingspan measured directly on the bird in the hand was 0.595 m. Tracings of the bird's wing were analysed using a digitizer table, which gave a wing area of 0.0593 m^2, including the area of the body between the wings. These measurements result in an aspect ratio (wingspan squared divided by wing area) for the fully stretched wing of 5.97. These measurements were used only when calculating predictions from aerodynamic equations (e.g. Pennycuick, 1975; Pennycuick, 1989; Tucker,

1987). Our conclusions on flight performance are based on the measurements derived from digital images captured in connection with every data point (see below). The body frontal area measured in flight was 0.0036±0.0001 m^2 (mean ± S.D., N=10). The body mass, m, was relatively stable between flight sessions (m=0.1844±0.0037 kg, mean ± S.D., N=66). The body mass at the beginning of all flight sessions ranged between 0.193 and 0.181 kg. To calculate the body mass for each data point, we interpolated from a straight line between the start and end mass for every flight session and used the mass corresponding to the time of measurement.

The flight feathers were in good condition throughout the experimental period. However, a few tail feathers were lost by breakage in the housing aviary. They were all replaced using thin insect needles inserted into the shaft of the feather and held in place with a tiny drop of superglue. It was not possible to discriminate between broken and intact tail feathers in flight or when analysing the images, so we do not believe that this had any significant effect on the results.

Physical properties

To standardise the airspeed measurements, all airspeeds given in this paper refer to equivalent airspeeds (V_e):

$$V_e = \sqrt{\frac{2q}{\rho_0}}, \qquad (13)$$

where q is dynamic pressure and ρ_0 is the value assumed for the air density at sea level in International Standard Atmosphere (1.225 kg m^{-3}). The true and equivalent airspeeds are only the same if the air density is ρ_0. The wind tunnel is situated close to sea level, and the differences will therefore be small. The air density varied only between 1.20 and 1.23 kg m^{-3} (see Table 1) throughout the experimental period. Furthermore, the variation in air pressure and temperature in the test section was quite small (Table 1).

Experimental protocol

During the period 30 March to 19 April 1999, the jackdaw was flown experimentally on 10 occasions. The experiments lasted on average approximately 2 h, ranging between 75 min and 3 h. During the experiments, the bird showed no signs of fatigue or abnormal stress. If the bird did not want to fly, it was free to land on the floor of the test section, which it never did.

To determine the minimum glide angles at different speeds, we set the forward speed to a value between 4 and 16 m s^{-1} in steps of 0.5 m s^{-1} and the tilt angle to the maximum 6.37 °. If the bird were able to glide at all at the set speeds, we tilted the tunnel back towards the horizontal in steps of 0.03 ° to a point where it was not able to glide. We then tilted the tunnel again gradually to determine the exact minimum tilt angle at which the bird could just glide steadily. This determined the minimum tilt angle for this particular forward speed and was entered as an independent observation. The jackdaw was able to glide at angles up to 6.37 ° between 6 and 11 m s^{-1}. To determine the lowest possible forward speed at maximum tilt angle, the tilt angle was pre-set and the forward speed was altered. This procedure was repeated six times over the whole speed range, generating a total of 66 measured points. Data were collected in a randomised sequence with at least 1.0 m s^{-1} between tested airspeeds in the same tidal sequence. From measurements of tilt angle and forward airspeed in the tunnel, the associated sinking speed was calculated according to equation 1.

Table 1. *Physical properties of the air during the experiments*

	Temperature (°C)	Air density (kg m^{-3})	Pressure (hPa)
Mean ± S.D. (N=66)	18.2±2.07	1.21±0.01	1016±11
Maximum	21.7	1.23	1028
Minimum	15.9	1.20	997

Photography

For every data point, an image was taken of the bird. To do this, we used a high-speed camera (RedLake MotionScope PCI 500) connected to a personal computer (WinNT 4.0) *via* a frame grabber. The camera was mounted below the test section, i.e. looking at the bird from below, on the external metal frame of the test section. This arrangement ensured that the camera was always perpendicular to the direction of the airflow as it moved with the tunnel when we tilted it up and down. To illuminate the bird, four 500 W light bulbs were used, also mounted on the outside frame of the test section to ensure similar light conditions between film sequences. The camera had a 4 mm lens and was set to grab 125 frames s^{-1} with the shutter open for 1/1875 s and an aperture of f=11.

When the bird was gliding steadily, a sequence of images was collected. From each sequence, we selected a single JPEG image to represent the performance at this particular combination of sinking and forward speeds. This approach also helped in deciding whether the bird was really gliding steadily as we captured a sequence. If there were any movements of the bird forwards or backwards within the tunnel, a new sequence was collected.

To measure the body frontal area, the bird was filmed from behind while flying actively at 11 m s^{-1}, and 10 JPEG images were captured and used for analysis. For maximum wingspan, the bird was filmed from below in horizontal flapping flight at 11 m s^{-1}. Five JPEG images were extracted in mid downstroke. We assumed that the wings were stretched fully in mid downstroke and used these measurements as a representative value of the maximum wingspan for calculations of span ratio, etc.

To analyses the JPEG images, we used Mapinfo Professional, version 4.5, which allows raster images to be imported and registered as maps, facilitating measurements of distance and area. On all 66 images, we measured the wing area, which includes the area between the wings, tail area and wingspan. To convert the image values of wing area and wingspan, we used a reference length from the tip of the tail

to the point where the leading edge of the wing meets the body (0.212 m).

The size of the images was 480 pixels×420 pixels, allowing high-resolution analysis. Each image was first zoomed so that part of a single pixel could be selected as a starting point. For wing area and tail area measurements, the perimeter of the wing was marked, including the indentations between single wing feathers. To measure the area of the body between the wings, a line was interpolated from the joint of the wing leading edge to the body on the left side to that on the right, and from the inner tertial on the right to that on the left side, resulting in one measurement for the whole wing area (see Pennycuick, 1989). The tail area was calculated as the area behind the interpolated line between the tips of the inner tertiaries and the area covered by the tail feathers, i.e. wing and tail area taken together occupies the whole projected bird apart from the neck and head. Wingspan was measured as a straight line between the outermost tips of the longest primaries. This was the case both for gliding flight and for the measurements of maximum wingspan on the images collected in flapping flight.

The body frontal area was calculated as the area occupied by the body as viewed from behind, using maximum wingspan as measured on the bird in flapping flight at 11 m s^{-1} as the reference length.

Results

Flight behaviour

The jackdaw usually moved longitudinally within the test section in a cyclic pattern in which it moved backwards and then accelerated forwards using a series of wing beats even though the tunnel was tilted (see Tucker and Heine, 1990). However, the bird did remain in equilibrium gliding flight for several seconds, sometimes for up to a minute, and during such episodes we recorded the wing and tail geometry. It was quite easy to judge when the bird was gliding at equilibrium and when it was not, but we also used the high-speed video cameras to select moments when the bird remained motionless with respect to the test section of the tunnel. The bird appeared to glide more comfortably at certain speeds, e.g. 8.5–10 m s^{-1}, as indicated by the duration and frequency of equilibrium gliding episodes. We were able to find a lowest tilt angle at which the bird would glide at equilibrium at all speeds between 6 and 11 m s^{-1}; outside this range, the maximum tilt angle of the tunnel prevented steady gliding. The feet were lowered at speeds of 8.0 m s^{-1} and below, but only at 6 m s^{-1} were they lowered at an angle of approximately 60 ° (measured from the horizontal) with the toes opened to maximise drag. At 6.5 m s^{-1}, the feet were partly closed and the tarsi were raised to approximately 45 °, and at 7 m s^{-1} the toes were fully closed, but still held in a position below the body. At 8.5 m s^{-1} and above, the feet were fully retracted and held close to the body. The tail was spread maximally at the lowest speed and was fully furled at 9.5 m s^{-1} and above.

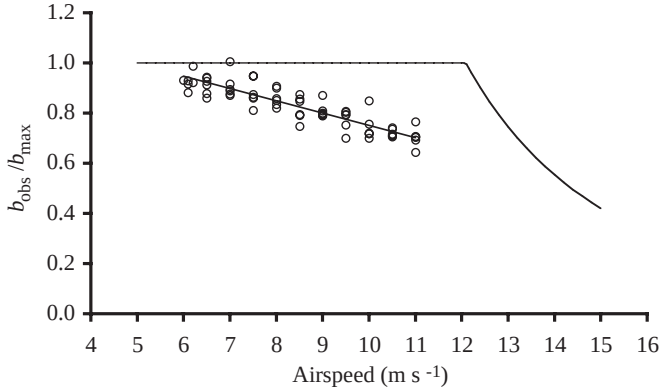

Fig. 2. Span ratio (b_{obs}/b_{max}) of the jackdaw, where b_{max} is 0.569 m, decreased linearly over the gliding flight speed range (b_{obs}/b_{max}=–0.0488V+1.239, N=66, r^2=0.79, P<0.01). The span ratio for the jackdaw, predicted from drag-minimising theory, is plotted for comparison (equation 12; Pennycuick, 1989).

Wingspan and wing area at different speeds and angles

By selecting a few variables such as wingspan, wing area and span ratio, it is possible to describe the most important properties of the wing planform in gliding flight.

The wingspan decreased linearly over the whole speed range, 6–11 m s^{-1} (b=–0.028V+0.705, N=66, r^2=0.79, P<0.01). The span ratio, expressed as the ratio of observed wingspan b_{obs} to maximal wingspan b_{max}, shows that the wing was only close to being fully stretched at the very lowest gliding speeds in our measurements (Fig. 2). Maximum wingspan during flapping flight was measured on the bird at 11 m s^{-1}, assuming that mid downstroke represents the full wingspan (Fig. 3; filled circles, b_{max}=0.569±0.008 m, mean ± S.D., N=5). The aspect ratio of the maximally stretched wing measured during flapping flight at 11 m s^{-1} was 5.62±0.08, mean ± S.D., N=5). Over the gliding flight speed range, the span ratio (b_{obs}/b_{max}), where b_{max} is 0.569 m, decreased linearly over the gliding flight speed range, 6–11 m s^{-1} (Fig. 2; b_{obs}/b_{max}=–0.0488V+1.2391, N=66, r^2=0.79, P<0.01). The theoretical optimal span ratio ($\hat{\beta}$), according to equation 12, is plotted for comparison in Fig. 2 with k=1.1 and $C_{D,pro}$=0.014 and using the wingspan and area measured on the bird in the hand (Table 2). The theoretical span ratio is maximal ($\hat{\beta}$=1) up to 12 m s^{-1}, after which it starts to decrease with further increases in airspeed.

Wing area increased with wingspan as measured on the bird in gliding flight (Fig. 3, open circles) and was best described by a second-degree polynomial. We also measured the wing area when manually flexing the wing on the bird and drawing sketches of the wing (Fig. 3, filled triangles). There was no significant difference between the two methods, indicating that the wing can be flexed only along one geometrical trajectory. For the manually flexed wing, the relationship between wing area and wingspan is described by S=0.0665b^2+0.0316b+0.0156 (Fig. 3; r^2=0.99, N=15, P<0.001). The maximum wing area observed in flapping flight at 11 m s^{-1} was 0.058±0.002 m^2 (mean ± S.D.).

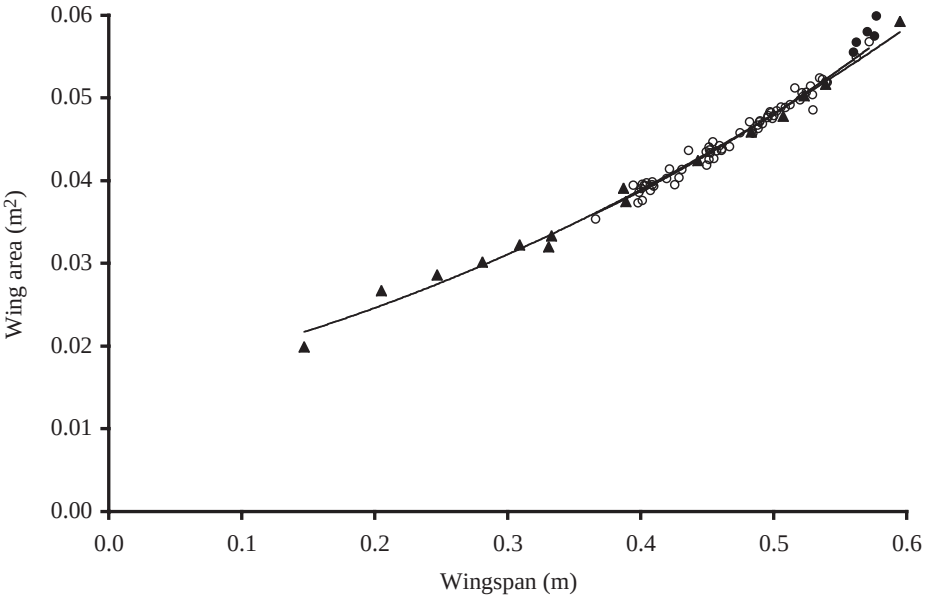

Fig. 3. The relationship between wingspan and wing area of the jackdaw. Open circles, values measured for the bird in gliding flight. Filled triangles, values measured when manually flexing the wing of the bird held in the hand. There was no significant difference between the two methods, indicating that the wing can be flexed only along one geometrical trajectory. For the manually flexed wing, the function of wing area (S) with respect to wingspan (b) is described by $S=0.0665b^2+0.0316b+0.0156$ ($r^2=0.99$, $N=15$, $P<0.001$). Filled circles represent maximum wingspan as measured for the bird in horizontal flapping flight at 11 m s^{-1} ($b=0.569\pm0.008$ m, mean ± S.D., $N=5$).

We also analysed the wing area ratio (ε) with respect to wingspan ratio (β) as shown in Fig. 4 for wingspan and area measured during flight ($N=66$). The slope δ of this relationship was 0.97 (reduced major axis regression, $\varepsilon=-0.014+0.97\beta$, d.f.=64), which did not differ significantly from unity (95 % confidence interval for the slope is 0.93–1.01).

Tail area at different speeds and glide angles

The tail was spread extensively at low and moderate speeds. At speeds between 6 and 9 m s^{-1}, the tail area (S_{tail}) decreased linearly with speed (Fig. 5; $S_{tail}=-0.0016V+0.0203$, $N=42$, $r^2=0.83$, $P<0.01$). However, above 9 m s^{-1}, we assume that the tail is completely folded and, hence, has the same area irrespective of speed (S_{tail} =0.0056±0.0004 m^2, mean ± S.D., $N=24$). The tail with maximum spread at 6.1 m s^{-1} (0.0115 m^2, $N=1$) had an area 2.1 times that of the completely folded tail.

Reynolds number

The dimensionless Reynolds number (Re) is the ratio between inertial and frictional forces and is an index accounting for the general size of the object affected by the air stream, airspeed and the properties of the fluid. It has effects on the flow pattern around the wings and, hence, also on the calculations performed of the coefficients of lift and drag (von Mises, 1945). The Reynolds number is defined as:

$$Re = \frac{Vl}{v}, \qquad (14)$$

where V is airspeed, l is a characteristic length of the object and v is the kinematic viscosity, i.e. the ratio of the viscosity to the density of the air.

As a representative length to calculate Re, we used the mean wing chord (c), i.e. the ratio of wing area to wingspan. The chord is normally assumed to be constant over a range of speeds, which seems to be a good assumption for the jackdaw data (Fig. 6A; $c=0.0002V+0.0948$, $N=66$, $r^2=0.03$, $P>0.05$). Re ranges from 38 000 at 6 m s^{-1} to 76 000 at 11 m s^{-1} using the mean chord measured for each data point (Fig. 6B).

The glide polar

The bird was flown at different speeds while the tilt angle was changed. In this way, we were able to define the

Table 2. *Data required for calculating stall speed and span ratio for three bird species studied in gliding flight in wind tunnels*

Species	b_{max} (m)	S_{max} (m^2)	m (kg)	$C_{L,max}$	V_{min} (m s^{-1})	β_e at V_{min}	β_e at $2V_{min}$
Jackdaw[1]	0.60	0.059	0.18	2.1	4.9	1	0.76
Harris' hawk[2]	1.02	0.190	0.70	1.6	6.1	1	0.78
Laggar falcon[3]	1.01	0.132	0.57	1.6	6.6	1	0.68

b_{max}, maximum wingspan; S_{max}, maximum wing area; m, body mass; $C_{L,max}$, maximum value of coefficient of lift; V_{min}, stall speed calculated according to equation 18 (see text); β_e, span ratio.

[1]Jackdaw in the present study, see text.

[2]Tucker and Heine, 1990.

[3]Tucker and Parrot, 1970; Tucker, 1987.

To obtain β_e at $2V_{min}$ for the Harris' hawk and laggar falcon, we have re-analysed published data.

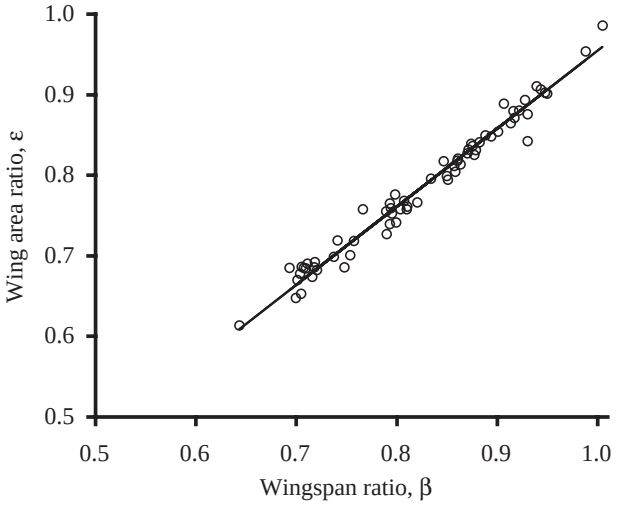

Fig. 4. Wing area ratio ($\varepsilon=S/S_{max}$) with respect to wingspan ratio ($\beta=b_{obs}/b_{max}$) for a jackdaw in gliding flight (N=66). The reduced major axis regression is $\varepsilon=-0.014+0.97\beta$, with a 95 % confidence limit for the slope of 0.93–1.01.

minimum sinking speed required for steady gliding flight at a given forward speed (Fig. 7). Fitting a polynomial regression equation to the data, the relationship is $V_s=0.0424V^2-0.624V+2.916$ (Fig. 7; solid line, N=66, r^2=0.91, P<0.002). This function results in a minimum sinking speed (V_{ms}) of 7.4 m s^{-1}, which is the forward speed associated with the minimum sinking rate, and a speed for best glide (V_{bg}) at 8.3 m s^{-1}, which is the speed associated with maximum lift:drag ratio. Minimum sinking speed (V_{ms}) corresponds to a sinking speed of 0.62 m s^{-1}. However, Pennycuick (Pennycuick, 1975) suggested that a function of the type:

$$V_s = \frac{\tau}{V} + \gamma V^3 , \qquad (15)$$

would be the appropriate form of a fixed-wingspan glide polar, where τ and γ represent different variables, such as wingspan, wing area, weight and other physical properties. The regression calculated for $1/V$ and V^3 with the intercept set to zero results in the expression:

$$V_s = \frac{2.83}{V} + 0.00064V^3 , \qquad (16)$$

which has a V_{ms} at 6.2 m s^{-1} and a V_{bg} at 8.2 m s^{-1}. V_{ms} corresponds here to a sinking speed of 0.61 m s^{-1}. This function is less curved than the polynomial regression equation, especially in the lower speed range, and has a slightly different position (Fig. 7; broken line, N=66, r^2=0.85, P<0.01).

We have also tried to fit the theory according to the super-polar for gliding flight performance proposed by Pennycuick (Pennycuick, 1989) to the jackdaw data by changing variables such as k, $C_{D,par}$ and $C_{D,pro}$ in combination with our observed data on wingspan ratio, b_{max}, S and S_b. However, we had limited success, and the best fit was no better than the fit obtained using the fixed-wingspan model (equation 16; Fig. 7).

Gliding flight performance: lift and drag

Lift and drag were calculated on the basis of body weight and the angle of the flight path with respect to the horizontal (equations 2 and 3; Fig. 1). The relationship between the ratio of lift to drag (L:D) and airspeed showed an inverted U-shape and reached a maximum of 12.6 at 8.5 m s^{-1} (Fig. 8; L:D=$-0.611V^2+10.43V-31.913$, r^2=0.67, N=66, P<0.01). The 95 % confidence limits for the maximum L:D ratio were 8.42 and 8.64 m s^{-1} for airspeed and 12.05 and 13.16 for the L:D ratio (Bootstrap analysis). To decompose total drag, we calculated induced drag according to equation 6, with the induced drag factor (k) set to 1.1, and subtracted it from total drag to visualise profile and parasite drag as a single combined component. Total drag shows a shallow U-shape with respect to speed, while induced drag decreases with speed and the combined profile and parasite drag increase with speed (Fig. 9).

The lift coefficients were calculated in two different ways using equation 4: (i) assuming the wing to be the only lift-generating surface according to conventional gliding flight theory (Fig. 10, solid line), and (ii) including the tail area in

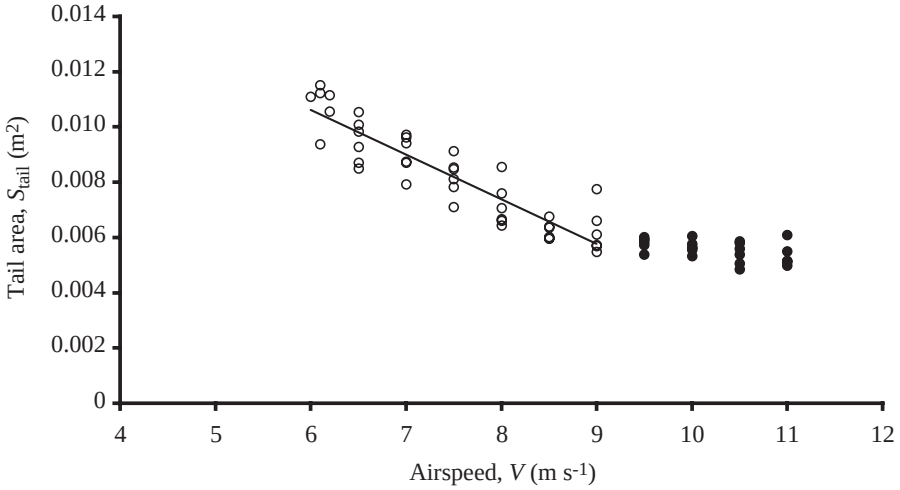

Fig. 5. Tail area S_{tail} with respect to airspeed V for a jackdaw in gliding flight. The tail area decreased linearly with speed between 6 and 9 m s^{-1} ($S_{tail}=-0.0016V+0.0203$, N=42, r^2=0.83, P<0.01). Above 9 m s^{-1}, the tail is completely folded and has the same area irrespective of speed (S_{tail}=0.0056±0.0004 m^2, mean ± S.D., N=24).

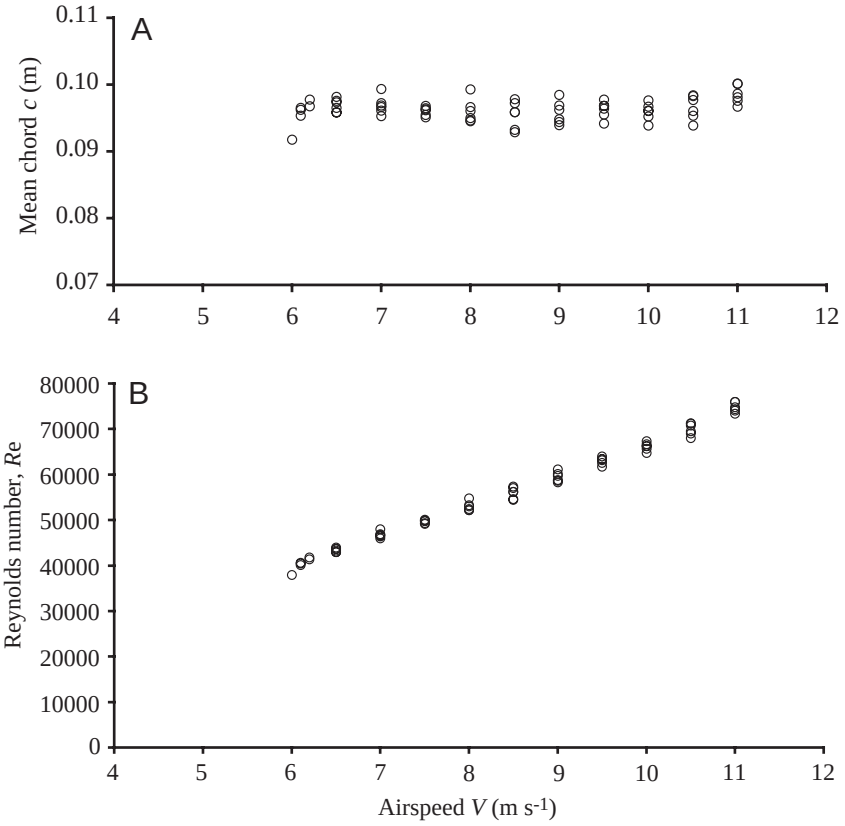

Fig. 6. (A) Mean chord *c* with respect to airspeed *V* for a jackdaw in gliding flight. The ratio of wing area to wingspan (mean chord) was not affected by airspeed (c=0.0002V+0.0948, N=66, r^2=0.03, P>0.05). (B) Reynolds number *Re* with respect to airspeed. *Re* was calculated for the mean chord of the wing and ranges from 38 000 at 6 m s^{-1} to 76 000 at 11 m s^{-1}.

the lift-generating surface (Fig. 10, broken line). The jackdaw spread its tail extensively at speeds up to 9 m s^{-1}, probably to generate additional lift. We included the tail area beyond the area of the completely folded tail in the lift-generating area when calculating lift coefficients (cf. Fig. 5). This means that the tail area at and above 9.5 m s^{-1}, where the tail is completely folded, was assigned the value of 0 and at and below 9.0 m s^{-1} the mean area of the folded tail was subtracted from the total tail area. At speeds above 9.0 m s^{-1}, the lift coefficients are therefore the same because the tail is completely folded, but with decreasing speed the lift coefficients will be lower than if not including the variable tail area (Fig. 10). At the lowest measured gliding speed (6.0 m s^{-1}), the uncorrected lift coefficient was 1.66 (N=1) and that with tail area correction was 1.49 (N=1). However, our estimates of maximum lift

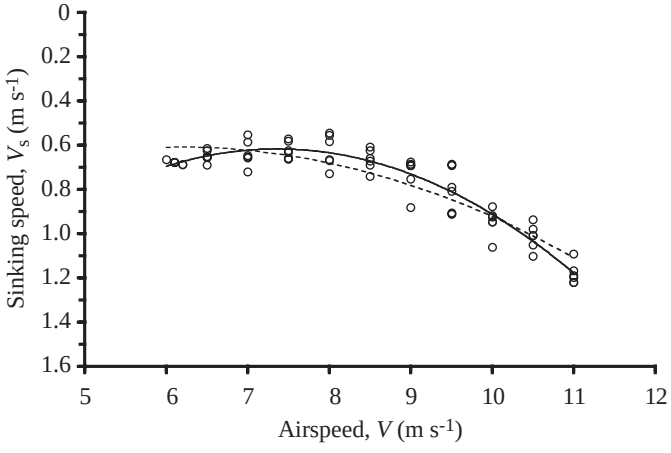

Fig. 7. Measured glide super-polar for a jackdaw. Each data point represents the minimum amount of sink (V_s) required for equilibrium gliding at a given forward speed V. The solid line shows the best fit by a polynomial regression: V_s=0.0424V^2–0.624V+2.916 (N=66, r^2=0.91, P<0.002), where V_s is sinking speed, and has an associated minimum sinking speed (V_{ms}) of 7.4 m s^{-1} and a speed for best glide (V_{bg}) of 8.3 m s^{-1}. If the model proposed by Pennycuick (Pennycuick, 1989) for the calculated fixed-wingspan glide polar is fitted to the data set (broken line), V_{ms} is 6.2 m s^{-1} and V_{bg} is 8.2 m s^{-1} (N=66, r^2=0.85, P<0.01).

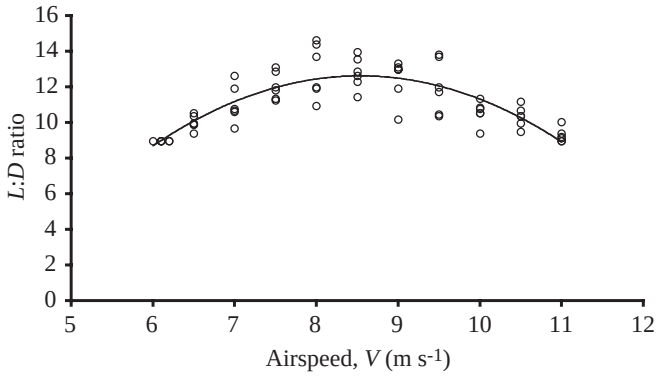

Fig. 8. The inverted U-shaped relationship between the ratio of lift to drag (L:D) and airspeed V reached a maximum of 12.6 at 8.5 m s^{-1} (L:D=–0.611V^2+10.43V–31.913, r^2=0.67, N=66, P<0.01). The 95 % confidence limits for the maximum are 8.42 and 8.64 m s^{-1} for airspeed and 12.05 and 13.16 for the L:D ratio (Bootstrap analysis).

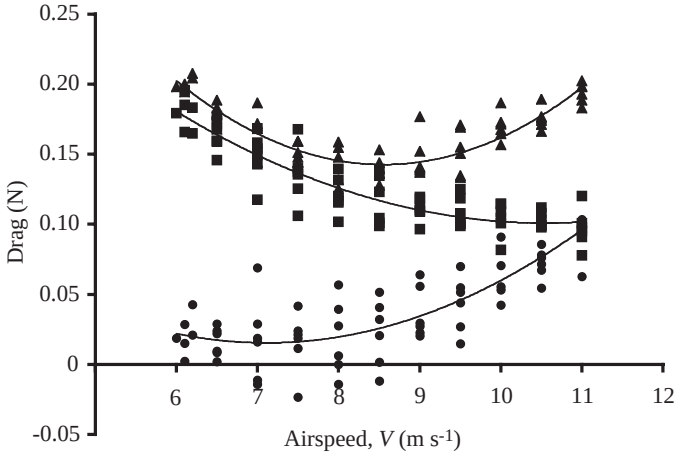

Fig. 9. Total drag and drag components with respect to airspeed for the jackdaw. Total drag (triangles) was calculated on the basis of body weight and the angle of the flight path with respect to the horizontal (see text). Induced drag (squares) was calculated according to equation 6. Induced drag was then subtracted from total drag (equation 9) to give the combined parasite and profile drag (circles).

coefficients should be considered conservative since we were unable to tilt the tunnel through angles steeper than 6.37° to check whether the jackdaw could glide steadily at even lower speeds. Hence, the stall speed could be at a slightly lower speed than 6 m s^{-1} and so the maximum coefficient of lift could be somewhat greater than 1.66. Even at the lowest steady speed, the jackdaw did not have its wings fully extended, which probably reflects the fact that the tunnel could not be tilted further to achieve the true minimum speed. Using the regression relationship between b_{obs}/b_{max} and speed (Fig. 2) and extrapolating to b_{obs}/b_{max}=1 gives a stall speed V_{min} of 4.9 m s^{-1} for the jackdaw (Table 2). Taking this as the true stall speed and using wing area only as the reference area, we calculated a $C_{L,max}$ of 2.07 from equation 18 (see below). We think that this value comes close to the maximum lift coefficient that a jackdaw can achieve at its minimum speed by splaying its primaries (Kokshaysky, 1977; Norberg, 1990).

New empirical equations for predicting span ratio, wingspan and wing area in gliding birds

In this section, we present a new equation for predicting wingspan and wing area for a bird in gliding flight at any speed, since our observations of the jackdaw did not comply with the minimum drag theory according to equation 12 (cf. Fig. 2). This is also true for two bird species investigated by others (see below) for which the observed data do not agree well with equation 12 either. When predicting the flight behaviour of a bird not previously studied in a wind tunnel, the data available are limited, and we will therefore base the equations on a reasonable estimate of the maximum lift coefficient, body mass, maximum wingspan and maximum wing area that can be measured for the bird in the hand (Pennycuick, 1989).

Apart from this study, there are a few studies available on birds in gliding flight for which wing morphology has been reported over the whole speed range investigated, including the laggar falcon *Falco jugger* (Tucker and Parrot, 1970; Tucker, 1987) and Harris' hawk *Parabuteo unicinctus* (Tucker and Heine, 1990). Tucker and Parrot (Tucker and Parrot, 1970) and Tucker and Heine (Tucker and Heine, 1990) explicitly reported data on span ratio and wing area over the speed range investigated for the falcon and hawk, respectively. The slopes of the linear regressions for the relationship between span ratio and airspeed are very similar for the two species (Fig. 11). The relationship between span ratio at stall speed (V_{min}) and span

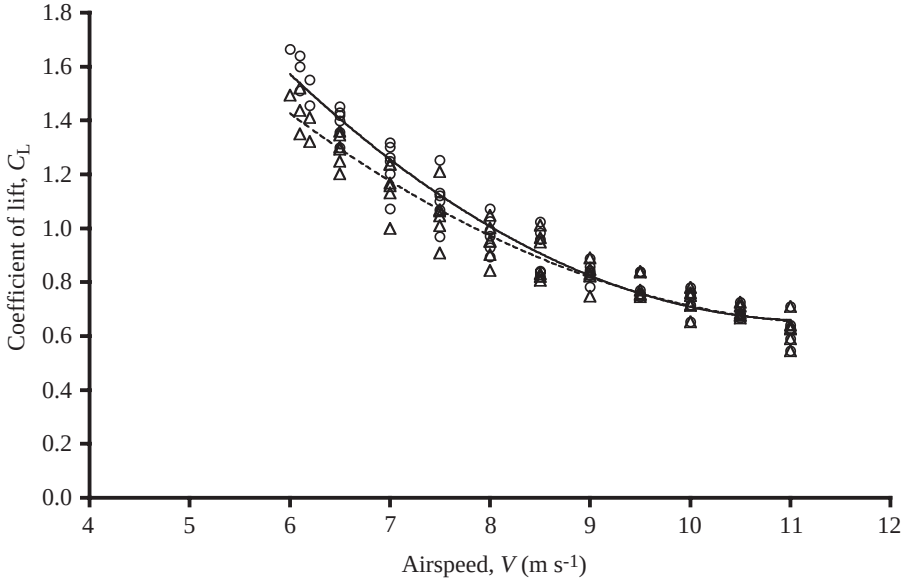

Fig. 10. The dimensionless force coefficients for lift (C_L; calculated according to equation 4) with respect to airspeed. Two different assumptions were made to calculate the coefficients. First, we assumed that the wing was the only lift-generating surface (solid line). Second, we included the tail area in the lift-generating surface (broken line). The added tail area was simply the extra area created by spreading the tail from its completely folded position; hence, the completely folded tail was considered to have zero area (see text). The jackdaw spread its tail extensively up to 9 m s^{-1} to generate additional lift and drag (cf. Fig. 5). At speeds above 9.0 m s^{-1}, the lift coefficients are the same using both assumptions because the tail is completely folded, but with decreasing speed the lift coefficients will be lower than if not including the variable tail area. At the lowest measured gliding speed (6.0 m s^{-1}), the uncorrected lift coefficient was 1.66 (N=1) and that with tail area correction was 1.49 (N=1).

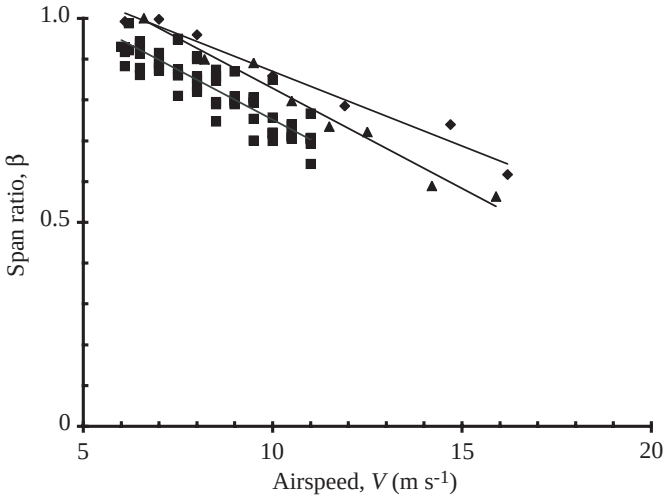

Fig. 11. Observed relationships between span ratio $\beta=b_{obs}/b_{max}$, and airspeed for three birds. Diamonds, Harris' hawk (Tucker and Heine, 1990); triangles, laggar falcon (Tucker and Parrot, 1970); squares, the jackdaw from the present study. The straight lines are regression lines, which explain between 79 and 98 % of the variation.

ratio at some multiple of V_{min}, for the different birds, is the variable we will use when predicting span ratio with respect to speed in gliding birds (Table 2). Span ratio predicted from our equation will be denoted 'β_e' (subscript e for empirical) not to be confused with $\hat{\beta}$ predicted from equation 12. We set β_e at V_{min} equal to 1 and calculated that β_e at $2V_{min}$ is approximately 3/4 for the three species (Table 2). Using this observation and assuming that there is a linear relationship between β_e and speed, we derived the following equation for span ratio as a function of speed:

$$\beta_e = \frac{5}{4} - \frac{V}{4V_{min}} . \quad (17)$$

The wingspan ratio is maximal (β_e=1) at V_{min}, i.e. the minimum airspeed at which the bird can produce enough lift for steady gliding flight. The stall speed is given by:

$$V_{min} = \sqrt{\frac{2mg}{\rho S C_{L,max}}} , \quad (18)$$

where the variables are as defined as above (see Table 2). Using the values given in Table 2, one can calculate the actual span ratio at any speed by using equations 17 and 18. Here, β_e decreases linearly with increasing speed until it reaches a minimum value of 1/3, hence $1/3 \leqslant \beta_e \leqslant 1$, since there is a minimum possible wingspan ultimately constrained by the diameter of the body. Observed minimum values for span ratios are somewhat higher than 1/3, but Pennycuick (Pennycuick, 1968) reports a minimum span ratio for a pigeon (*Columba livia*) very close to 1/3. Using equation 17 to calculate β_e, the wingspan can then be calculated as:

$$b = \beta_e b_{max} , \quad (19)$$

where b_{max} is the maximum wingspan measured on the bird.

There is a weak parabolic (cf. Fig. 3; Tucker and Heine, 1990) near-linear relationship between wing area and wingspan (Tucker and Parrot, 1970). For simplicity, we will assume a linear relationship between wing area and wingspan. The mean chord (c) of the wing is assumed to stay unchanged with speed (see Fig. 6A), linking wingspan and wing area:

$$c = \frac{S_{max}}{b_{max}} = \frac{S}{b} , \quad (20)$$

where the variables are as defined as above. By combining equation 19 and 20, it is possible to calculate the wing area at any speed as:

$$S = c\beta_e b_{max} . \quad (21)$$

This approach allows, with information about $C_{L,max}$, b_{max}, S_{max} and m, wing area and wingspan to be calculated at any forward gliding speed, for any bird. In Fig. 12, we compare the predictions of the relationship between wing area and wingspan with observed relationships for the falcon, hawk and jackdaw from calculated V_{min} to 20 m s^{-1}. The small discrepancy between the observed and predicted values must be attributed to the approximations of the relationships between speed and wing morphology and the assumption that c is constant.

If we use equation 9 and exchange b and S with a wingspan and wing area, respectively, that change with speed according to equations 17, 19 and 21, we can calculate an alternative gliding flight super-polar based on the actual wingspan and wing areas observed for birds in wind tunnels (as opposed to the super-polar for which the span ratio is calculated according to equation 12). We did this for a bird with the dimensions of a jackdaw and superimposed the two alternative super-polars

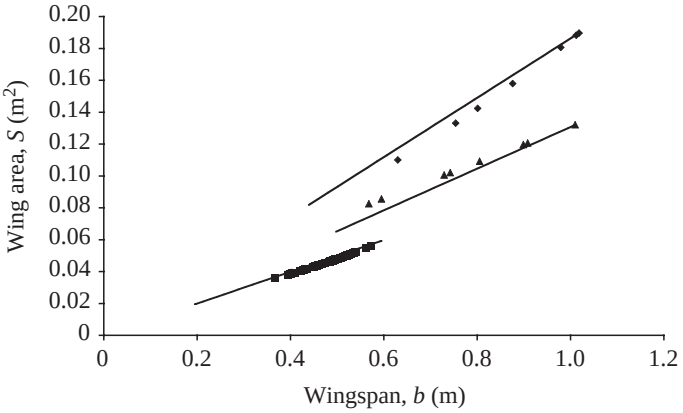

Fig. 12. Predicted and observed relationships between wing area and wingspan in three species: Harris' hawk (diamonds), laggar falcon (triangles) and jackdaw (squares). Symbols are observed values and straight lines are the predictions from calculated stall speed to 20 m s^{-1} for each bird based on body mass, maximum wingspan, maximum wing area and maximum coefficient of lift (see Table 2). Underlying assumptions are a constant chord, a linear relationship between wing area and wingspan, $\beta_e(V_{min})$=1 and $\beta_e(2V_{min})$=3/4, where β_e is the span ratio and V_{min} is stall speed.

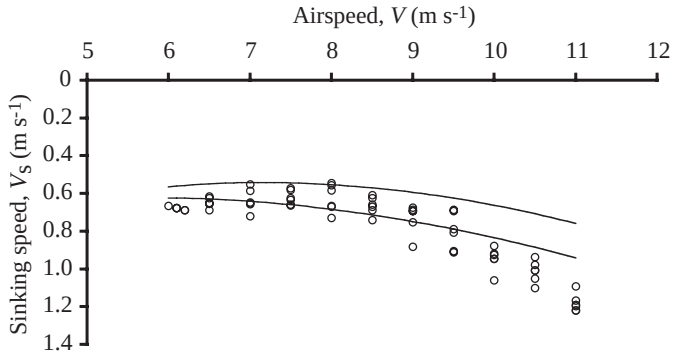

Fig. 13. Maximum performance during forward gliding flight for a jackdaw flying in a windtunnel. The upper curve is the maximum performance curve calculated according Pennycuick (Pennycuick, 1989) and using equation 12 to calculate the wingspan ratio. The lower curve is calculated according to the same theory, but instead using equations 17, 19 and 21 to calculate wingspan and area at different speeds. Parameter valued were k (induced drag factor)=1.1, $C_{D,par}$ (parasite drag coefficient)=0.1 and $C_{D,pro}$ (profile drag coefficient)=0.014.

on the jackdaw data (Fig. 13). We compared a glide super-polar calculated from equation 9, using equations 17, 19 and 21, with that of the super-polar calculated using equation 12 for span ratios minimising induced and profile drag. For both curves, we assumed a body drag coefficient $C_{D,par}$ of 0.1 (Pennycuick et al., 1996), k=1.1 and $C_{D,pro}$=0.014. Using equations 17, 19 and 21, we obtained a better fit to the data than when using wingspan ratio calculated according to equation 12 (see Fig. 13). We suggest that the default value for $C_{L,max}$ if no information is available for an arbitrary bird species should be 1.8 (see Table 2).

Discussion

The range of speeds for which the jackdaw could glide steadily in the wind tunnel was 6–11 m s^{-1}, i.e. a rather limited range compared with that known to be achieved by birds of similar size (see Pennycuick, 1968). This was due only to the limitation of angles through which the wind tunnel could be tilted. At the lowest speed range, we found a maximum lift coefficient $C_{L,max}$ of 1.66 or 1.49, depending on whether the tail was included in the lift-generating surface or not. It is likely, however, that the jackdaw is capable of achieving a still higher C_L since the wings were not fully extended and showed no tendency to stall at the lowest speed measured, perhaps by further splaying of the primaries (cf. Kokshaysky, 1977; Norberg, 1990). In the equations for predicting wingspan and wing area, we have assumed a value of $C_{L,max}$ of 2.1 for the jackdaw, which corresponds to a stall speed of 4.9 m s^{-1}. In any case, our values of $C_{L,max}$ are similar to those found for other species gliding in wind tunnels (see Table 2; Pennycuick, 1968; Pennycuick, 1971c; Tucker and Parrot, 1970; Tucker and Heine, 1990).

Tucker (Tucker, 1988) reports lift coefficients of up to 2.2 in free-flying African white-backed vultures *Gyps africanus*. Tucker (Tucker, 1993) found that, in wings with slotted wingtips, induced drag can be reduced by vertical spreading of the vortices shed at the wingtip compared with a wing without such slots. The maximum lift to drag ratio was 12.6±0.55 (mean ±95 % confidence interval) at 8.5 m s^{-1} in the jackdaw, which is near the speed for the best glide ratio, as calculated from the polynomial regression for the data points on the glide super-polar (V_{bg}=8.3 m s^{-1}, associated with a sinking speed of 0.62 m s^{-1} to give a glide ratio of 13.4:1). Ideally, the maximum lift to drag ratio should be equal to the best glide ratio, but the discrepancy found here can be attributed to measurement errors and to small variations in body mass between test sessions. In comparison with the pigeon (Pennycuick, 1968), the jackdaw appears to be better adapted for efficient gliding flight. In fact, it shows a maximum lift to drag ratio slightly higher than that of the Harris' hawk (Tucker and Heine, 1990), but substantially lower than that of albatrosses (Idrac, 1924; Pennycuick, 1982).

An interesting feature of the jackdaw was the near-linear relationship between wingspan and speed, such that the wingspan was near maximal only at the lowest speed and then decreased linearly with increasing speed. This was clearly at variance with the expected behaviour if the bird were to minimise induced and profile drag (equation 12; Pennycuick, 1989). We therefore re-examined previous data published in support of such a prediction of span ratio in gliding flight (Pennycuick, 1968; Parrot, 1970; Tucker and Parrot, 1970; Tucker, 1987; Tucker and Heine, 1990). For four species for which wingspan has been measured with respect to speed, three (pigeon, laggar falcon and Harris' hawk) showed a near-linear reduction starting at low speeds, similar to that of the jackdaw, while the fourth species (black vulture *Coragyps atratus*) showed no reduction with increasing speed. For two of the species, values for span ratios were given explicitly in the literature, allowing the data to be re-examined (laggar falcon and Harris' hawk). The relationships between span ratio at stall speed (V_{min}) and span ratio at some multiple of V_{min} were very similar for the different species (Table 2), and the straight-line regressions in Fig. 11 explain between 79 and 98 % of the variation in the three data sets.

We tried, with little success, to modify equation 12 to fit the observed behaviour assuming that the drag-minimising concept is correct, but that the relative magnitudes of the different drag components, induced and profile drag, might be wrong. One explanation is that induced drag has been overestimated and that the wings of a bird are capable of producing sufficient lift with submaximal wingspan at most speeds. Flexing the wings, thereby reducing the wingspan and area, would then minimise the profile drag at all speeds. The induced drag factor (k) is usually set at 1.1 for gliding flight. Raspet (Raspet, 1960) and Cone (Cone, 1962) (cited in Pennycuick, 1971b) did suggest that values of k even lower than 1 (k=1 is the value for a wing with perfectly elliptical lift distribution) could be achieved in birds with slotted wings (see also Tucker, 1995). The derivation of equation 12 assumed that

the planform slope (δ) is 1 and, in fact, it was not significantly different from 1 for the jackdaw. The variables in the denominator of the right-hand side of equation 12 are fairly well defined and should not have caused the discrepancy. One change that would shift the speed downwards where β=1 is that the dependence of speed itself should be stronger than $V^{-0.75}$. Consequently, a stronger dependence on speed could mean that profile drag increases more strongly with increasing speed than is currently believed.

The attempt to fit equation 12 to the observed span reduction in the three bird species with these modifications failed. We suggest, therefore, that the model for predicting span ratios according to equation 12 should be rejected with respect to the available data. Instead of using equation 12, we propose that equations 17, 19 and 21 should be used when calculating gliding flight super-polars in birds, using for example the software supplied by Pennycuick (Pennycuick, 1989). This approach to calculating β_e is based on the few studies available for which wingspan over a speed range has been measured and explicitly given in the literature, and it therefore represents an entirely empirical basis for this proposition. It would, of course, be desirable to find an aerodynamic explanation for the observed linear reduction in wingspan with increasing speed related to that proposed by Tucker (Tucker, 1987). The variable with the lowest reliability in this model is probably $C_{L,max}$, which has been shown to be hard to measure accurately (Tucker and Heine, 1990).

We have also tried to give a simple equation to calculate wing area for a bird given information about its maximum wingspan, mean chord and β_e (equation 21). This equation gives predictions reasonably close to the observed values (see Fig. 12), but there are still some small discrepancies that can be attributed to the small error in the assumed relationship between wing morphology and speed. However, our aim is to propose a set of equations requiring a minimum number of variables to give a reasonable prediction that can be used for any species. By measuring a bird's body mass, maximum wingspan and corresponding wing area according to Pennycuick (Pennycuick, 1989), and assuming a value for the maximum coefficient of lift, it is possible to estimate the wingspan and wing area at any speed for a bird. These morphological data can then be used to calculate the super-polar for gliding flight (Fig. 13), for example using the programs supplied by Pennycuick (Pennycuick, 1989). The use of equations 17, 19 and 21 to estimate wingspan and area, rather than equation 12, gives an improved fit with data for the jackdaw in gliding flight. However, by studying more species, it should be possible to obtain more accurate estimates of $C_{L,max}$ and of the relationship between β_e and speed and, ultimately, also better predictions from a modified flight model.

List of symbols

b	wingspan
b_{max}	maximum wingspan
b_{obs}	observed wingspan
c	wing chord
$C_{D,pro}$	profile drag coefficient
$C_{D,par}$	parasite drag coefficient
C_L	lift coefficient
$C_{L,max}$	maximum lift coefficient
D	drag force
D_{ind}	induced drag force
D_{par}	parasite drag force
D_{pro}	profile drag force
$\boldsymbol{g}$	acceleration due to gravity
k	induced drag factor
L	lift force
l	length
m	body mass
q	dynamic pressure
Re	Reynolds number
S	wing area
S_b	body frontal area
S_{max}	maximum wing area
S_{tail}	tail area
V	speed
V_{bg}	speed for best glide ratio
V_e	equivalent air speed
V_{min}	stall speed
V_{ms}	speed for minimum sink
V_s	sinking speed
β	span ratio (b_{obs}/b_{max})
$\hat{\beta}$	optimal span ratio, minimising total drag
β_e	empirical span ratio
δ	planform slope
ε	wing area ratio (S/S_{max})
γ	a parameter
ν	kinematic viscosity
π	the ratio of the circumference to the diameter of a circle
θ	angle
ρ	air density
ρ_0	air density at sea level in International Standard Atmosphere ($1.225\,kg\,m^{-3}$)
τ	α parameter

We are grateful to Lennart Blomquist and Kenneth Bengtsson for catching the jackdaw. We are also grateful to Colin Pennycuick for constructive comments on an earlier version of this paper and to Kirsty Park for help with the Bootstrap analysis. An anonymous referee provided careful and constructive criticism that significantly improved the paper. This research was supported by the Swedish Natural Science Research Council and Carl Tryggers Foundation to A.H.

References

Hedenström, A. (1993). Migration by soaring or flapping flight in birds: the relative importance of flight cost and speed. *Phil. Trans. R. Soc. Lond. B* **342**, 353–361.

Hummel, D. (1992). Aerodynamic investigations on tail effects in birds. *Z. Flugwissenschaften Weltraumsfirschung* **16**, 159–168.

Idrac, M. P. (1924). Contributions à l'étude duvol des albatros. *C.R. Acad. Sci. Paris* **179**, 28–30.

Kokshaysky, N. V. (1977). Some scale dependent problems in aerial animal locomotion. In *Scale Effects in Animal Locomotion* (ed. T. J. Pedley), pp. 421–435. London: Academic Press.

Norberg, U. M. (1990). *Vertebrate Flight.* Berlin: Springer-Verlag.

Parrott, C. G. (1970). Aerodynamics of gliding flight of a black vulture *Coragyps atratus. J. Exp. Biol*. **53**, 363–374.

Pennycuick, C. J. (1968). A wind-tunnel study of gliding flight in the pigeon *Columba livia*. *J. Exp. Biol.* **49**, 509–526.

Pennycuick, C. J. (1971a). Soaring behaviour and performance of some east African birds, observed from a motor-glider. *Ibis* **114**, 178–218.

Pennycuick, C. J. (1971b). Gliding flight of the white-backed vulture *Gyps africanus. J. Exp. Biol.* **55**, 13–38.

Pennycuick, C. J. (1971c). Gliding flight of the dog-faced bat *Rousettus aegyptiacus* in a wind tunnel. *J. Exp. Biol.* **55**, 833–845.

Pennycuick, C. J. (1975). Mechanics of flight. In *Avian Biology* (ed. D. S. Farner and J. R. King), pp. 1–75. New York: Academic Press.

Pennycuick, C. J. (1982). The flight of petrels and albatrosses (Procellariiformes), observed in South Georgia and its vicinity. *Phil. Trans. R. Soc. Lond. B* **300**, 75–106.

Pennycuick, C. J. (1989). *Bird Flight Performance: A Practical Calculation Manual*. Oxford: Oxford University Press.

Pennycuick, C. J., Alerstam, T. and Hedenström, A. (1997). A new low-turbulence wind tunnel for bird flight experiments at Lund University, Sweden. *J. Exp. Biol.* **200**, 1441–1449.

Pennycuick, C. J., Klaassen, M., Kvist, A. and Lindström, Å. (1996). Wing beat frequency and the body drag anomaly: wind tunnel observations on a thrush nightingale (*Luscinia luscinia*) and a teal (*Anas crecca*). *J. Exp. Biol.* **199**, 2757–2765.

Raspet, A. (1960). Biophysics of bird flight. *Science* **132**, 191–200.

Spaar, R. and Bruderer, B. (1996). Soaring migration of steppe eagles *Aquila nepalensis* in southern Israel: flight behaviour under various wing and thermal conditions. *J. Avian Biol.* **27**, 289–301.

Spaar, R. and Bruderer, B. (1997). Optimal flight behaviour of soaring migrants: a case study of migrating steppe buzzards, *Buteo buteo vulpinus. Behav. Ecol.* **8**, 288–297.

Spedding, G. R. (1987). The wake of a kestrel *Falco tinnunculus* in gliding flight. *J. Exp. Biol*. **127**, 45–57.

Thomas, A. L. R. (1993). On the aerodynamics of birds' tails. *Phil. Trans. R. Soc. Lond. B* **340**, 361–380.

Tucker, V. A. (1987). Gliding birds: the effect of variable wingspan. *J. Exp. Biol.* **133**, 33–58.

Tucker, V. A. (1988). Gliding birds: descending flight of the white-backed vulture, *Gyps africanus*. *J. Exp. Biol.* **140**, 325–344.

Tucker, V. A. (1992). Pitching equilibrium, wingspan and tail span in a gliding Harris' hawk, *Parabuteo unicinctus. J. Exp. Biol.* **165**, 21–41.

Tucker, V. A. (1993). Gliding birds: reduction of induced drag by wing tip slots between the primary feathers. *J. Exp. Biol.* **180**, 285–310.

Tucker, V. A. (1995). Drag reduction by wing tip slots in a gliding Harris' hawk, *Parabuteo unicinctus. J. Exp. Biol.* **198**, 775–781.

Tucker, V. A., Cade, T. J. and Tucker, A. E. (1998). Diving speeds and angles of a gyrfalcon (*Falco rusticolus*). *J. Exp. Biol.* **201**, 2061–2070.

Tucker, V. A. and Heine, C. (1990). Aerodynamics of gliding flight in a Harris' hawk, *Parabuteo unicinctus*. *J. Exp. Biol.* **149**, 469–489.

Tucker, V. A. and Parrot, G. C. (1970). Aerodynamics of gliding flight in a falcon and other birds. *J. Exp. Biol.* **52**, 345–367.

von Mises, R. (1945). *Theory of Flight*. New York: McGraw-Hill. (Dover edition, 1959).

Withers, P. C. (1981). The aerodynamic performance of the wing in red-shouldered hawk *Buteo linearis* and a possible aeroelastic role of wing-tip slots. *Ibis* **123**, 239–247.